DOI: 10.1002/chem.201001600

Host–Guest Inclusion Compound from Nitramine Crystals Exposed to Condensed Carbon Dioxide

Sabine Saint Martin,[a] Samuel Marre,[a] Philippe Guionneau,[a] François Cansell,[a] Joel Renouard,[b] Virginie Marchetto,[b] and Cyril Aymonier*[a]

Abstract: HNIW or CL20 (2,4,6,8,10,12-hexanitro-2,4,6,8,10,12-hexaazaisowurtzitane) is a nitramine, which is considered as the highest energetic molecular compound known to date, therefore, attracting increasing interest in propulsion applications. Additionally, CL20 is an interesting system for fundamental studies, exhibiting several polymorphs, which can behave as host lattices for trapping guest molecules. Herein, a new CL20 structure that contains inserted CO_2 molecules is reported. A combination of Fourier transform infra red (FTIR) spectroscopy, scanning electron microscopy (SEM), single-crystal X-ray diffraction, and thermal analyses (thermogravimetric analysis coupled with mass spectrometry and differential scanning calorimetry) was used to characterize this new material.

Keywords: energetic materials · host–guest systems · inclusion compounds · nitramines · X-ray diffraction

Introduction

Host–guest inclusion compounds, defined as complexes in which one chemical compound (host) forms cavities in which molecules of a second compound (guest) are located, have been known and studied for years.[1,2] Some of the most well-known host systems are supramolecular organic materials, such as cyclodextrins[2,3] and calixarenes,[4] which are of particular interest to selectively trap small organic molecules for enantiomer separation and recognition,[5] active substance delivery,[6] or polymerization in matrices.[7] Organic crystals as guests for host molecules[8] are yet another example of these complex systems, being considered as a prototype example of multicomponent self-organization.[9] Similar to what can be observed with atoms in inorganic solid-state chemistry, guest molecules trapped within host organic crystal lattices can induce deformation of the d spacings and/or rearrangement of the molecules.[10] These inclusions and further modifications of the host organic crystal often end up with changes in the material characteristics, which can lead to benefits through the appearance of new interesting properties, or to a loss of the initial characteristics of the crystal.

There has been increasing interest in studying energetic materials inclusion compounds,[11] because their polymorphism is a crucial parameter that influences many of their properties[12] and their use in propulsion applications. Most applications seek the most stable polymorph that exhibits the highest energy and mass density at ambient conditions, because the detonation velocity increases proportionally with density.[13] Among these materials HNIW (2,4,6,8,10,12-hexanitro-2,4,6,8,10,12-hexaazaisowurtzitane), also known as CL20, which is one of the most energetic materials, was developed in recent years.[14]

The crystalline structure of CL20 can behave as a host lattice for small molecules. CL20–guest inclusion compounds are generally obtained during crystallization processes. For instance, it was reported that CL20 can trap solvent molecules, such as disulfolane,[15] methanol,[16] or *N*,*N*-dimethylformamide (DMF).[17] This latter adduct is the only clathrate compound that has been characterized by single-crystal X-ray measurement; it exhibits a CL20/DMF molar ratio of 1:2 and crystallizes in a triclinic system ($P\bar{1}$ space group). The authors assumed the molecules are linked by van der Waals interactions, whereas no hydrogen bonding or dipolar interaction exist within the adduct.[17] Additionally, other small molecules, such as dimethylsulfoxide (DMSO) (form-

[a] Dr. S. Saint Martin, Dr. S. Marre, Prof. P. Guionneau, Prof. F. Cansell, Dr. C. Aymonier
CNRS, Université de Bordeaux, ICMCB
87 Avenue du Dr. A. Schweitzer, 33608 Pessac (France)
Fax: (+33) 540-002-761
E-mail: aymonier@icmcb-bordeaux.cnrs.fr

[b] J. Renouard, V. Marchetto
SNPE Matériaux Energétiques
Avenue Gay Lussac, 33167 Saint-Médard-en-Jalles (France)

ing a 1:1 complex), dioxane (3:2 complex), γ-butyrolactone (2:1 complex), and hexamethylphosphoramide (3:1 complex) have also been reported to form molecular complexes with CL20, but have not been characterized by X-ray diffraction (XRD).[18]

Photolytic and thermal decompositions are yet other ways to form CL20 inclusion compounds, because several gaseous products generated from its gentle decomposition are observed within CL20 crystals.[16] For instance, electron paramagnetic resonance measurements of the decomposition of CL20 indicate that NO_x products are trapped within the crystal lattice at extremely low temperatures and atmospheric pressure, and these compounds remain stable for extended periods of time at room temperature. This stability suggests the formation of clathrate with near-neighbor molecules that form an inclusion site.[19] One amongst the other decomposition products of CL20 is CO_2, which was identified as a guest molecule within CL20 crystal lattices during the heating and simultaneous decomposition of a particular polymorph of CL20 (ε-CL20).[20] However, except Fourier transform infra red spectroscopy (FTIR) analysis, no report to date is made about any characterization of the potential new inclusion compound CL20–CO_2.

Herein, we demonstrate the formation of a CL20 inclusion compound from the exposure of ε-CL20 crystals to condensed carbon dioxide, leading to the formation of a new CL20–CO_2 structure. Through the combination of different characterization techniques, such as FTIR spectroscopy, scanning electron microscopy (SEM), XRD, and thermal analyses—thermo gravimetric analysis coupled to mass spectrometry (TGA-MS) and differential scanning calorimetry (DSC)—the inclusion of CO_2 molecules within the CL20 crystal lattice is investigated. Finally, the characteristics of this new CL20–CO_2 host–guest material are presented.

Results and Discussion

The novel CL20–CO_2 inclusion compound is prepared by contacting ε-CL20 crystals with condensed carbon dioxide at high pressures (up to 16 MPa), at temperatures ranging from 20 to 80 °C, and with various contacting times (2 to 24 h) by using a high pressure set-up detailed elsewhere.[21] More details are given in the Experimental Section.

CL20 exhibits three anhydrous polymorphs (ε, β, and γ) and one hydrate form (α), which are presented in Figure 1: ε-CL20—considered in this study—is the polymorph of CL20 with the highest mass density, γ-CL20 is the thermodynamically stable form at high temperature, which is obtained from heating either ε-, α-, or β-CL20.[20] Another reported polymorph, the high pressure ζ-CL20 phase, was discovered from a reversible phase transition from the γ-phase, however, it was not yet characterized by XRD.[22]

FTIR spectroscopy studies: The obtained CL20–CO_2 crystals were first characterized by FTIR spectroscopy. Typical spectra taken before and after exposure of CL20 to condensed CO_2 (2 h, 15 MPa, 80 °C) are presented in Figure 2. A strong absorption band centered at 2345 cm^{-1} appears in the spectra of the crystals exposed to CO_2 (Figure 2a). This band can be assigned to the antisymmetric stretching vibration of CO_2. However, it appears to be shifted to lower wavenumber by about 15 cm^{-1} compared to the free CO_2 molecules absorption band, generally located at 2360 cm^{-1} (Figure 2b).

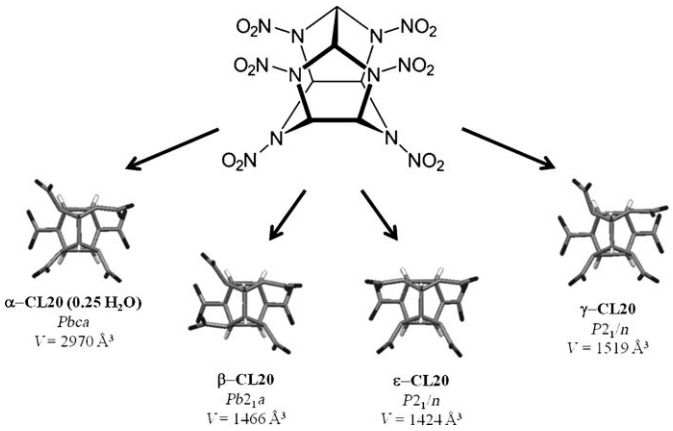

Figure 1. The CL20 molecule and its different known conformations: α-, β-, ε-, and γ-CL20. White, red, blue, and gray stands for H, O, N, and C atoms, respectively, *V* is the cell volume.[15]

This slight difference indicates that the CO_2 molecules do not have the same free motion as in the gas phase, which results from the modification of their environment through intermolecular interactions with surrounding CL20 molecules. Nevertheless, such a small shift suggests that the CO_2 molecules remain linear within this inclusion compound.

When considering the 1200–700 cm^{-1} region of the spectra (Figure 2c), generally defined as the CL20 polymorph IR "fingerprint",[23] the CL20–CO_2 spectrum exhibits slight differences compared to the ε-CL20 starting material, however, it can be easily superposed with the IR spectrum of α-CL20, suggesting that a phase transition to the alpha phase has occurred. The similarity between IR spectra of the α-CL20 (hydrate form of CL20) and CL20–CO_2 suggests that CO_2 is located into similar inclusion sites as H_2O within the α-CL20 lattice. The main differences between spectra of CL20–CO_2 and α-CL20 are observed in the wavenumber regions of 3075–3000 cm^{-1} and 1670–1520 cm^{-1}, typical for C–H stretching and NO_2 vibration modes, respectively (Figure 2d and e).[24] These differences can be explained by a different environment for the hydrogen atoms and probable interaction between the CO_2 molecules and the NO_2 groups of CL20 in CL20–CO_2.

Although CO_2 can be adsorbed on the crystal surface of CL20, the IR spectra strongly suggest that CO_2 mostly penetrates into the bulk, leading to a solid-state transformation. Further investigations have been performed to determine the thermal stability of the CL20–CO_2 inclusion compound.

Thermal investigations: TGA-MS and DSC measurements have been carried out in order to study the behavior of the

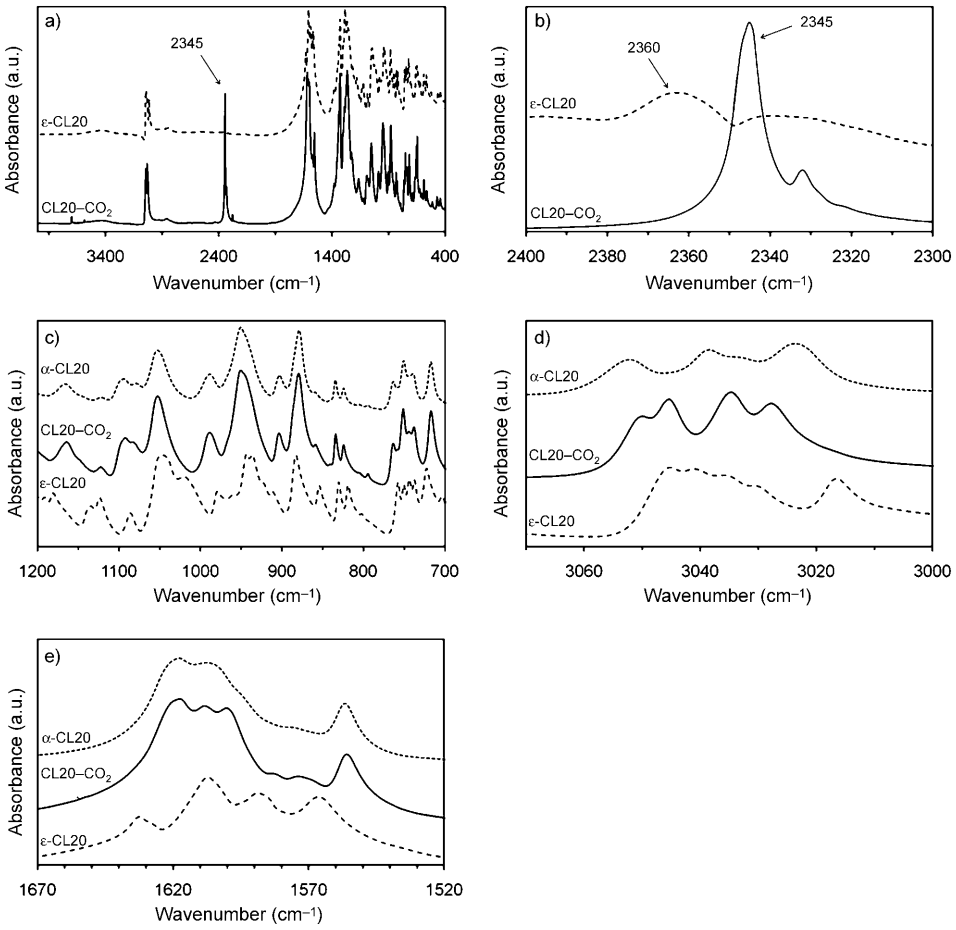

Figure 2. Different wavenumber regions of the IR spectra of ε-CL20, CL20–CO_2, and α-CL20: a) comparison of ε-CL20 and CL20–CO_2 in the range of 4000–400 cm^{-1}; b) comparison of the antisymmetric vibration modes of trapped CO_2 in the CL20–CO_2 structure and gaseous CO_2; c), d), and e) comparison of ε-CL20, CL20–CO_2, and α-CL20 in the range of 1200–700 cm^{-1}, 3075–3000 cm^{-1}, and 1670–1520 cm^{-1}, respectively.

CL20–CO_2 inclusion compound upon temperature change (Figure 3). The DSC analysis shows an endothermic phenomenon in the temperature range 160–200 °C, which corresponds to a solid–solid phase transition from the CL20–CO_2 to the γ-CL20 polymorph, followed by an exothermic phenomenon above 210 °C due to thermal decomposition of the γ-CL20 polymorph (Figure 3a).[20,25] TGA-MS characterization displays two weight-loss signals in the same temperature ranges (i.e., 160–200 °C and above 210 °C, Figure 3b). The mass to charge ratio (m/z) of 44 that corresponds to CO_2, demonstrates that CO_2 molecules are released during the solid–solid phase transition (Figure 3c). Therefore, the CO_2 insertion within the CL20 crystal lattice is stable for temperatures up to 160 °C, beyond which temperature CO_2 is released.

Crystal morphology: The initial CL20 crystals are aggregated and twinned crystals, with a large particle size distribution. Two kinds of starting materials were used. The first sample consists of particles with an average size of 30–50 μm (S1, Figure 4a), whereas the second sample contains particles with an average size of 250–400 μm (S2, Figure 4b; crystal sizes are evaluated considering the pyramid height). In both cases, the crystals have irregular pyramid shape with smooth surfaces.

The surface aspect of the crystals after exposure to CO_2 (sharp edges, smooth surface) indicates that the CL20 crystals have not undergone any modification under these conditions. Although the particle size distributions and the shapes are not affected by the exposure to condensed CO_2 (2 h, 15 MPa, 80 °C), several fractures appear on the surface of the crystals, likely induced by stress cracking of the CL20 crystals (Figure 4c and d).

Structural investigation: Single-crystal X-ray diffraction has been carried out for determining the structure of this new inclusion compound. The results confirm the insertion of CO_2 within the CL20 crystal lattice, which shows that exposure to condensed CO_2 transforms the monoclinic lattice of ε-CL20 into an orthorhombic lattice that has similar parameters to that of α-CL20 (Table 1). Thus, the insertion of CO_2 within ε-CL20 leads to a α-CL20-type phase, which, therefore, we have named α-CL20–CO_2.

Table 1. Comparison of the unit cell parameters and the density values of ε-CL20 at 150 K,[26] α-CL20–0.5 CO_2 at 150 K and α-CL20–0.25 H_2O at 293 K.[15]

	ε-CL20	α-CL20–CO_2	α-CL20–H_2O
space group	*P*21/*n*	*Pbca*	*Pbca*
a [Å]	8.800(1)	9.6895(6)	9.485(2)
b [Å]	12.499(1)	13.210(1)	13.225(4)
c [Å]	13.299(1)	23.515(2)	23.673(3)
β [°]	106.62	90	90
V [Å^3]	1401.7	3010.0	2969.5
ρ_{calcd}	2.076	2.031	1.980

The unit cell of α-CL20–CO_2 is composed of four CO_2 molecules per eight CL20 molecules, which occupy centrosymmetric cavities within the α-CL20 structure and are located on the inversion centers of this structure (Figure 5a). In comparison, the unit cell of α-CL20–H_2O contains eight CL20 molecules and two H_2O molecules, which are located

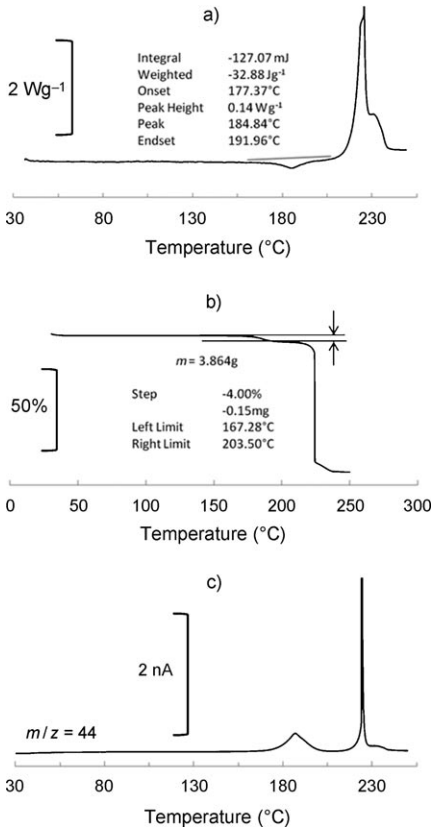

Figure 3. Thermograms of a ε-CL20 sample after exposure to condensed CO_2: a) DSC, b) TGA, and c) MS analysis, respectively.

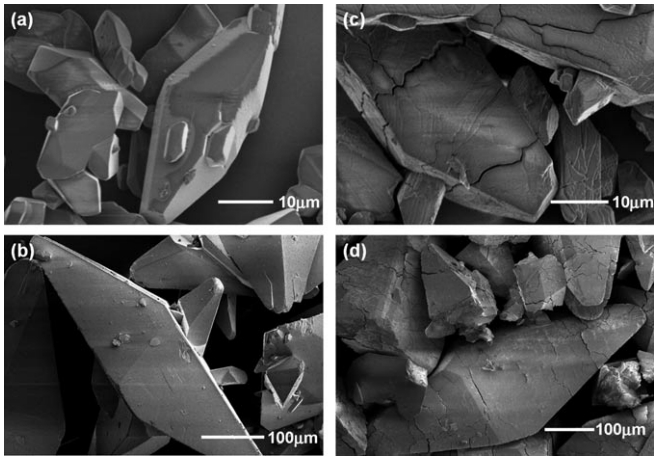

Figure 4. SEM micrographies of ε-CL20 initial powders S1 (a) and S2 (b) and of the CL20–CO_2 crystals obtained after the exposure to condensed CO_2 for S1 (c) and S2 (d).

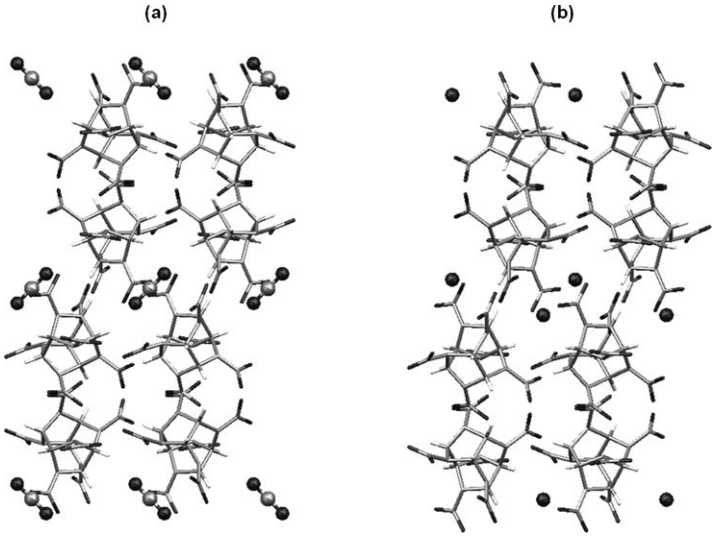

Figure 5. Comparison of the crystal lattice structure of the unit cells of a) α-CL20–CO_2 and b) α-CL20–H_2O.

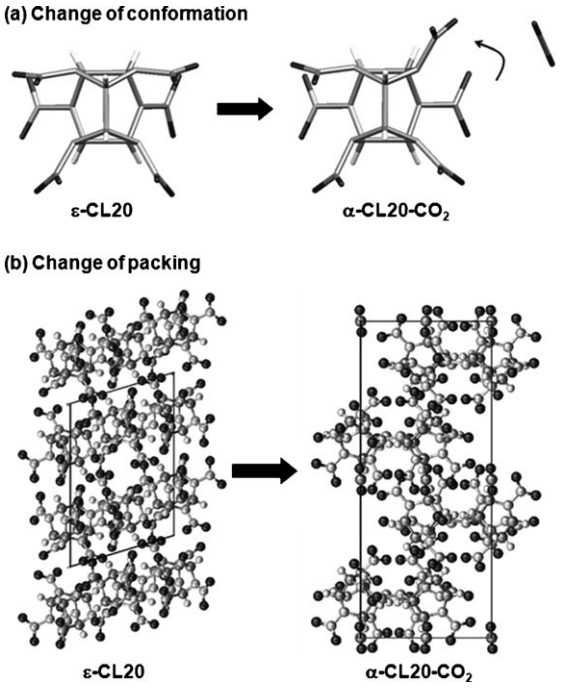

Figure 6. Representation of the main changes that occurred during the inclusion of CO_2 into the CL20 crystal lattice.

on both sides of the inversion centers (Figure 5b). Therefore, CO_2 and H_2O do not occupy exactly the same position in the two structures and have not the same occupancy rate.

As depicted in Figure 6, the insertion of CO_2 leads to a solid-state transformation, which results in two main changes: first, a conformer transition that is induced by the interaction of two nitramine groups with CO_2 (Figure 6a), then, a change of the orientation of the molecules into a reticular plane induces the transformation from a monoclinic to an orthorhombic lattice (Figure 6b).

The PLATON[27] software was used to estimate the available free volume of these two structures. Calculations are based on geometrical considerations from crystallographic data gained at 150 K for ε-CL20 and α-CL20–CO_2 and at 293 K for α-CL20–H_2O. The results show that ε-CL20 and α-CL20 exhibit cavities of $\approx$39 Å^3 and $\approx$63 Å^3, respectively.

Considering that the volume of an H_2O molecule is commonly admitted to be about 40 Å^3 and that the volume of a CO_2 molecule is larger, we conclude that ε-CL20 voids are too small to accommodate CO_2 inclusion.

Assumptions can be made concerning the stabilization of the CO_2 molecules within the CL20 crystal lattice by looking at intermolecular distances. Analysis of the CO_2 environment in the α-CL20–CO_2 structure reveals that the shortest distances between CL20 and the CO_2 molecules are located between the O atoms of CO_2 and the hydrogen atoms of CL20 with 2.54(1) Å at the origin of the van der Waals interaction (Figure 7). To a lesser extent, another short distance of 2.89(1) Å between CL20 and the CO_2 molecules corresponds to other van der Waals interaction between the $C^{\delta+}$ atom of CO_2 and the $O^{\delta-}$ atom of the NO_2 groups.

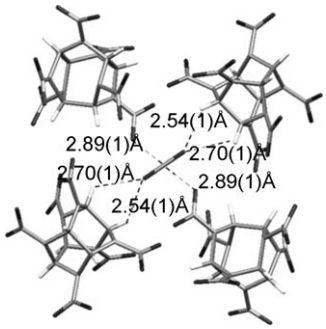

Figure 7. CO_2 stabilization into the α-CL20-CO_2 crystal lattice.

Conclusion

A new inclusion compound, α-CL20–CO_2, was synthesized by exposing ε-CL20 crystals to condensed carbon dioxide. Characterization by FTIR spectroscopy revealed the presence of CO_2 molecules. XRD confirmed the formation of an α-type CL20–CO_2 inclusion compound, which shows no noticeable change in CO_2 content over months or upon temperature treatment. To the best of our knowledge, this is the first time that the complete characterization of this compound is reported. The α-CL20–CO_2 crystals were obtained without any dissolution/precipitation process in organic solvents. The inclusion compound is obtained in the solid state through pressure-driven CO_2 insertion in the CL20 crystal lattice, which induces a transition from the ε-phase to the α-phase.

Experimental Section

Materials: **CAUTION**! CL20 is an explosive material highly sensitive to shock, heating, or static electricity. Small-scale and upgraded safety practices are strongly recommended. CL20 powders were obtained from SNPE Matériaux Energétiques with a certified purity of 95 wt% of ε-CL20 as indicated by IR characterization. Two grades were used for experiments: one with a specified particle size range between 30–50 μm (S1) and another one with a specified particle size range between 250–400 μm (S2). CO_2 (99.998% purity grade from Air Liquide) was used as received.

Apparatus and procedures: Safety warning: Experiments with condensed CO_2 are performed at high pressure and should be carried out with appropriate equipment. The set-up used to form CL20–CO_2 consists of a high-pressure reactor (255 cm^3) made of 316 stainless steel equipped with a pressure sensor and a thermocouple. In a typical experiment, ε-CL20 powder (≈500 mg) is introduced at the bottom of the reactor. The reactor is further closed, pressurized, and heated to the desired temperature. CO_2 is pumped by a feeding system composed of a CO_2 tank, a cooling apparatus, a high pressure pump (constant flow rate of 0.73 L h^{-1}), and a preheater that allows the fluid to be at the same temperature as inside the reactor. Once the operating conditions are reached inside the reactor (T, p), the conditions are maintained for a fixed period of time (t_c). Finally, the reactor is cooled, the purge valve is opened in order to slowly depressurize the system, and powders are collected at the bottom of the reactor.

FTIR spectroscopy: IR spectra were taken through KBr pellets (Ø = 10 mm) made by pressing a fine powder mixture consisting of CL20 powder (2 mg) and of dry KBr powder (200 mg) under a pressure of about 10 tons cm^{-2}. The spectra were taken with 4 cm^{-1} resolution in the range 4000–500 cm^{-1} by using a Thermo Electron Corporation (Nicolet 380 FTIR) Fourier transform IR interferometer, and data were collected and analyzed by using the EZ OMNIC software.

Scanning electron microscopy: Samples were characterized with a JEOL JSM-6390LV, allowing observation of the CL20 crystals despite their poor surface conductivity. Special sample preparation has been performed by using a JEOL SM-09010 cross-section polisher (ion beam mills) in order to observe crystals cross-sections.

Thermogravimetric analyses: TGA-MS and DSC experiments were carried out by using a TGA/DSC1 Mettler calorimeter coupled to a PFEIFFER mass spectrometer. Experiments were conducted under an argon atmosphere (Alphagaz 1 quality) as buffer gas (40.0 mL min^{-1}). Samples between 2–5 mg, weighted with a METTLER TOLEDO precision balance (±0.001 mg), are placed in aluminum pans and were heated from room temperature to 250 °C with a heating rate of 3 °C min^{-1}.

Single-crystal data collection: Colorless small prismatic single crystals with approximate size of 10 μm were coated in oil. To ensure sufficient diffraction peaks, Bragg peaks intensities were collected at 150(2) K by using a Rigaku Rapid R-axis diffractometer with a MM007 microfocus rotating anode generator with Cu radiation. The structural determination by direct methods and the refinement of atomic parameters based on full-matrix least squares on F^2 were performed by using the SHELX-97 programs[28] within the WINGX package.[29] The crystal structure is of average quality due to the weak number of observed Bragg peaks due to the alteration of the crystal quality during the ε-CL20-to-α-CL20-CO_2 transition.

[$C_6H_{12}N_{12}O_{12}$]·0.5 H_2O: a = 9.6895(6), b = 13.210(1), c = 23.515(2) Å, V = 3010.0(4) Å^3, d_{calcd} = 2.031, orthorhombic, space group *Pbca*, 2922 unique reflections (R_{int} = 0.15) for 287 refined parameters, R_{obs} = 0.080, $wR2_{obs}$ = 0.15, $(\Delta/\sigma)_{max}$ = 0.000, largest difference peak and hole 0.32/−0.31 e A^{-3}. CCDC-771863 contains the supplementary crystallographic data for this paper. These data can be obtained free of charge from The Cambridge Crystallographic Data Centre via www.ccdc.cam.ac.uk/data_request/cif.

Acknowledgements

The authors thank H. Graindorge, C. Marraud, S. Bénazet, G. Jacob, O. Dabard, C. Franson, N. Quaglia, F. Stankiewicz, and M. S. Amiet for the attention they have attached to this work. Prof. J. M. Léger is acknowledged for giving access to the rotating anode generator. K. Nagy is acknowledged for validating the English of the final version of the manuscript. Financial support from DGA, the French armament procurement agency, and SME, SNPE Matériaux Energétiques is gratefully acknowl-

edged. Many thanks to SME for the access to the "Centre de Recherches du Bouchet" and the "Etablissement de Saint Médard".

[1] a) F. Herbstein, *Crystalline Molecular Complexes and Compounds, Vol. 2*, Oxford University Press, New York, **2005**; S. G. Frank, *J. Pharm. Sci.* **1975**, *64*, 1585–1604; b) M. D. Hollingsworth, *Curr. Opin. Solid State Mater. Sci.* **1996**, *1*, 514–521.
[2] A. Sopková, *J. Inclusion Phenom. Mol. Recognit. Chem.* **1992**, *14*, 5–17.
[3] a) F. Giordano, C. Novak, J. R. Moyano, *Thermochim. Acta* **2001**, *380*, 123–151; b) W. Saenger, *Angew. Chem.* **1980**, *92*, 343–361; *Angew. Chem. Int. Ed. Engl.* **1980**, *19*, 344–362.
[4] a) A. Ikeda, S. Shinkai, *Chem. Rev.* **1997**, *97*, 1713–1734; b) H. Otsuka, Y. Suzuki, A. Ikeda, K. Araki, S. Shinkai, *Tetrahedron* **1998**, *54*, 423–446; c) U. Radius, *Z. Anorg. Allg. Chem.* **2004**, *630*, 957–972.
[5] a) R. Arad-Yellin, B. S. Green, M. Knossow, *J. Am. Chem. Soc.* **1980**, *102*, 1157–1158; b) G. Tsoucaris, G. Lebas, N. Rysanek, F. Villain, *J. Inclusion Phenom.* **1987**, *5*, 77–84.
[6] a) K. V. Shaitan, Y. V. Tourleigh, D. N. Golik, M. P. Kirpichnikov, *J. Drug Delivery Sci. Technol.* **2006**, *16*, 253–258; b) J. X. Zhang, P. X. Ma, *Angew. Chem.* **2009**, *121*, 982–986; *Angew. Chem. Int. Ed.* **2009**, *48*, 964–968; c) J. X. Zhang, H. L. Sun, P. X. Ma, *ACS Nano* **2010**, *4*, 1049–1059.
[7] a) J. Storsberg, H. Ritter, *Macromol. Rapid Commun.* **2000**, *21*, 236–241; Z. Li, F. W. Fowler, J. W. Lauher, *Abstr. Pap. Am. Chem. Soc.* **2006**, *231*, 206-ORGN; R. Arshady, K. Mosbach, *Macromol. Chem. Phys.* **1981**, *182*, 687–692.
[8] A. J. Cruz-Cabeza, G. M. Day, W. Jones, *Chem. Eur. J.* **2009**, *15*, 13033–13040; K. Nakano, K. Sada, M. Miyata, *Chem. Commun.* **1996**, 989–990; K. Nakano, K. Sada, K. Nakagawa, K. Aburaya, N. Yoswathananont, N. Tohnai, M. Miyata, *Chem. Eur. J.* **2005**, *11*, 1725–1733.
[9] J. Bordello, B. Reija, W. Al-Soufi, M. Novo, *ChemPhysChem* **2009**, *10*, 931–939; R. M. Yebeutchou, F. Tancini, N. Demitri, S. Geremia, R. Mendichi, E. Dalcanale, *Angew. Chem.* **2008**, *120*, 4580–4584; *Angew. Chem. Int. Ed.* **2008**, *47*, 4504–4508; F. G. Klärner, J. Benkhoff, R. Boese, U. Burkert, M. Kamieth, U. Naatz, *Angew. Chem.* **1996**, *108*, 1195–1198; *Angew. Chem. Int. Ed. Engl.* **1996**, *35*, 1130–1133; M. D. Ward, A. M. Pivovar, *Curr. Opin. Solid State Mater. Sci.* **1999**, *4*, 581–586; H. J. Choi, M. P. Suh, *J. Am. Chem. Soc.* **1998**, *120*, 10622–10628; S. S. Sun, A. J. Lees, *J. Am. Chem. Soc.* **2000**, *122*, 8956–8967.
[10] N. Hayashi, Y. Mazaki, K. Kobayashi, *Adv. Mater.* **1994**, *6*, 654–656; Y. Murakami, Y. Hisaeda, J. Kikuchi, T. Ohno, M. Suzuki, Y. Matsuda, T. Matsuura, *J. Chem. Soc. Perkin Trans. 2* **1988**, 1237–1246.
[11] L. E. Fried, M. R. Manaa, P. F. Pagoria, R. L. Simpson, *Annu. Rev. Mater. Res.* **2001**, *31*, 291–321.
[12] C. J. Eckhardt, A. Gavezzotti, *J. Phys. Chem. B* **2007**, *111*, 3430–3437.
[13] L. Borne, J. C. Patedoye, C. Spyckerelle, *Propellants Explos. Pyrotech.* **1999**, *24*, 255–259; M. H. Keshavarz, *J. Hazard. Mater.* **2005**, *121*, 31–36; M. H. Keshavarz, R. T. Mofrad, R. F. Alamdari, M. H. Moghadas, A. R. Mostofizadeh, H. Sadeghi, *J. Hazard. Mater.* **2006**, *137*, 1328–1332; V. V. Sil′vestrov, *Combust. Explos. Shock Waves (Engl. Transl.)* **2006**, *42*, 472–479.
[14] R. L. Simpson, P. A. Urtiew, D. L. Ornellas, G. L. Moody, K. F. J. Scribner, D. M. Hoffman, *Propellants Explos. Pyrotech.* **1997**, *22*, 249–255.
[15] A. T. Nielsen, A. P. Chafin, S. L. Christian, D. W. Moore, M. P. Nadler, R. A. Nissan, D. J. Vanderah, R. D. Gilardi, C. F. George, J. L. Flippen-Anderson, *Tetrahedron* **1998**, *54*, 11793–11812.
[16] M. D. Pace, *Mol. Cryst. Liq. Cryst.* **1992**, *219*, 139–148.
[17] Y. X. Ou, H. P. Jia, B. R. Chen, Y. J. Xu, J. T. Chen, R. X. Xu, *Chin. J. Org. Chem.* **1999**, *19*, 500–507.
[18] X. Zhao, J. Liu, Molecular complexes of hexanitrohexaazaisowurtzitane, *Vol. 16*, Beijing Ligong Daxue Xuebao, **1996**, pp. 494–497.
[19] M. D. Pace, *J. Phys. Chem.* **1991**, *95*, 5858–5864; L. R. Ryzhkov, J. P. Toscano, *Cryst. Growth Des.* **2005**, *5*, 2066–2072.
[20] T. P. Russell, P. J. Miller, G. J. Piermarini, S. Block, *J. Phys. Chem.* **1993**, *97*, 1993–1997.
[21] S. Marre, F. Cansell, C. Aymonier, *Nanotechnology* **2006**, *17*, 4594–4599.
[22] T. P. Russell, P. J. Miller, G. J. Piermarini, S. Block, *J. Phys. Chem.* **1992**, *96*, 5509–5512.
[23] M. F. Foltz, *Propellants Explos. Pyrotech.* **1994**, *19*, 63–69; E. von Holtz, D. Ornellas, M. F. Foltz, J. E. Clarkson, *Propellants Explos. Pyrotech.* **1994**, *19*, 206–212.
[24] Y. Kholod, S. Okovytyy, G. Kuramshina, M. Qasim, L. Gorb, J. Leszczynski, *J. Mol. Struct.* **2007**, *843*, 14–25.
[25] M. F. Foltz, C. L. Coon, F. Garcia, A. L. Nichols, *Propellants Explos. Pyrotech.* **1994**, *19*, 133–144.
[26] N. B. Bolotina, M. J. Hardie, R. L. Speer, A. A. Pinkerton, *J. Appl. Crystallogr.* **2004**, *37*, 808–814.
[27] A. L. Spek, *J. Appl. Crystallogr.* **2003**, *36*, 7–13.
[28] G. M. Sheldrick, *Acta Crystallogr. Sect. A* **2008**, *64*, 112–122.
[29] L. J. Farrugia, *J. Appl. Crystallogr.* **1999**, *32*, 837–838.

Received: June 7, 2010
Published online: October 11, 2010

